Experimentally Determined Rocket-Exhaust Flowfield in a Constrictive Tube Launcher

John J. Bertin*
University of Texas at Austin, Austin, Texas
and
James L. Batson†
U. S. Army Missile Command, Huntsville, Ala.

Pressure histories have been obtained during a flight test program in which a 6.0-in (15.2-cm) diameter rocket was launched from instrumented tube launchers whose cross section varied. Pressure measurements were used to define the flow mechanisms characterizing the underexpanded, supersonic rocket exhaust flow in the constrictive tube launcher. As the exhaust flow impinged on the constriction, the local pressure rose immediately, resulting in a pressure gradient in the annular region between the rocket and the launcher wall and, hence, the blowby flow. Later, when the rocket exhausted into the large-diameter forward tube, the flow was choked by the constrictive change in cross section and a normal shock wave was generated in the forward tube. Neither the geometry of the constriction nor the presence of vent ports significantly affected the pressure distribution in the launcher.

Nomenclature

p = static pressure
p_{tl} = total pressure in rocket stagnation chamber
r_{ne} = exit-plane radius of conical nozzle
r^* = throat radius of nozzle
x = axial distance with respect to face of modified rectangular step
$\bar{x}$ = axial distance from aft end of launch tube

Subscript

ne = location of nozzle-exit plane

Introduction

THERE are a variety of rockets that are launched from tubes which have a changing cross section. Because the cross section varies, the rocket is constrained immediately after ignition but, once it has sufficient velocity, it flies free of any tube support for a short distance as it emerges from the tube. A complex flowfield results when the rocket exhaust flow encounters the constrictive change in cross section of the so-called "nontipoff" launch tubes. The flow of the high-temperature and high-pressure exhaust gas is of practical interest in the structural design of the launcher and is of concern in connection with the possible generation of unbalanced forces on the rocket which could influence the trajectory.

When the rocket exhausts directly into the small-diameter aft tube, the flow downstream of the nozzle exit is entirely supersonic and intersecting, weak shock-waves occur. The resultant flowfield is that for an underexpanded, supersonic jet exhausting into a constant-area tube having an inside diameter which is slightly larger than the nozzle exit. Fabri and Siestrunk[1] found that the flowfield in the tube varied with increasing rocket chamber pressure from mixed flow (subsonic and supersonic flow exist in the tube) with flow separation in the tube to fully developed supersonic flow throughout the tube (except, of course, in the viscous layers). Batson[2] found that the static wall-pressure distributions in a constant-area tube which were obtained during a cold-gas test program were qualitatively similar to those obtained when a stationary rocket was exhausted into a constant-area tube. Batson and Bertin[3] examined the tube-wall static-pressure distributions which were obtained when a rocket accelerated through an instrumented tube. The static wall pressures from these dynamic rocket firings were qualitatively similar to the corresponding data from the static rocket firings of Ref. 2.

Significant blowby flow (i.e., exhaust gases which are directed upstream into the annular region between the rocket and the launcher wall) was observed during an eight-flight-test program in which Rip-Zap configurations were launched from a sparsely instrumented, nontipoff launch tube. The constrictive launch tube, the launcher instrumentation, and the resultant data are described in Ref. 4.

To aid in the analysis of the data from the Rip-Zap launch program, two additional test programs have been conducted in which an underexpanded jet of cold gas exhausted into a constrictive launch tube. The objectives of the cold-gas tests conducted at the U. S. Army Missile Command included the determination of the effect of reservoir pressure, nozzle-exit position, and constrictive geometry on the blowby mass-flow rate and on the static wall-pressure distribution in the launcher. The data from these tests were discussed in Ref. 5. When the nozzle exhausted directly into the small-diameter aft tube, there was no significant blowby flow. However, when the exhaust flow impinged on the constriction, significant blowby flow was generated. For many test conditions, the blowby flow in the annular region between the rocket and the launcher wall was transonic.

The objectives of the cold-gas test program conducted at the University of Texas at Austin included the determination of the effect of vent ports located just upstream of the constriction in the large-diameter forward tube. It was found[6] that the presence of vent ports (for the geometries considered) had no significant effect on the static wall-pressure distribution.

Discussed here in detail are the pressure measurements from a series of four flights in which Rip-Zap configurations were launched from a densely instrumented nontipoff tube launcher. The instrumentation package included static wall

Received December 22, 1974; revision received April 28, 1975. This work was supported by the U. S. Army Missile Command, through Contract DAAHO1-73-C-1016.

Index catagories: Jets, Wakes, and Viscid-Inviscid Flow Interactions; LV/M Configuration Design.

*Associate Professor, Department of Aerospace Engineering and Engineering Mechanics. Member AIAA.

†Engineer, U. S. Missile Research, Development and Engineering Laboratory. Member AIAA.

pressures, pitot pressures, and differential measurements of diametrically opposed static wall pressures. A primary objective of this flight-test program was to obtain information which could be used to define important parameters for the flowfield in the launcher. Of special interest was the identification of the source of the blowby flow. The data from the flight-test program are also compared with the data from the complementary cold-gas test programs.[5,6]

Test Program

During this test program, 4 Rip-Zap rockets were launched from nontipoff, constrictive launch-tubes, as shown in Fig. 1. The overall length of the rocket assembly (which consisted of a 4:1 ogive forward section powered by a Zap motor) was 130.23 in. (330.78 cm). The rocket, whose outside diameter was nominally 6.0 in. (15.2 cm), was initially constrained in its travel by sabots, which rode on the tube walls. Once the aft end of the rocket cleared the small-diameter aft tube, the supporting sabots dropped off, allowing the rocket to fly freely in the forward tube. The rocket gases exhausted from a conical nozzle having a half angle of 10°22'. Values for other parameters which characterize the supersonic exhaust flow were

$$r_{ne} = 2.833 \text{ in. } (7.196 \text{ cm})$$

$$r^* = 1.545 \text{ in. } (3.924 \text{ cm})$$

$$\gamma \approx 1.18, \text{ and}$$

$$P_{tl} \approx 1400 \text{ psia } (9.66 \times 10^6 \text{ N/m}^2)$$

The launcher, which had an overall length of 148.60 in. (377.44 cm), consisted of two launch tubes, which were assembled so that the aft tube had an inside diameter of 6.75 in. (17.15 cm) and the forward tube had an inside diameter of 8.75 in. (22.23 cm). As shown in Fig. 2, two different geometries were used to accomplish the constrictive change in cross section. A modified rectangular step was used for Flights 9 and 10, while a 15° ramp was used for Flights 11 and 12. The face of the rectangular step, which was 80.05 in. (203.33 cm) from the aft end of the launch tube, served as the origin for the dimensionless axial coordinate-system

$$x/r_{ne} = (80.05 - \bar{x})/2.833$$

Thus, as indicated in Fig. 2c, a negative value of the dimensionless axial coordinate corresponds to a location in the large-diameter forward tube of the launcher.

Another parameter of the experimental program was the presence (or absence) of access vent ports, which were located in the large-diameter forward tube for most of the test firings. For Flights 9, 10, and 11, there were 4 vent ports, 2 of which were located at $\bar{x}=82.99$ in. (210.79 cm) and 2 of which were located at $\bar{x}=84.25$ in. (214.00 cm). The paired vent ports were diametrically opposed at ϕ of 90° and 270°. Sketches of the vent ports and their location are presented in Fig. 3. Even with 4 ports, the vent area was less than 9% of the cross-sectional area of the (downstream) aft tube. Thus, as verified by the data of Ref. 6, the presence of vent ports did not appreciably change the static-presssure distribution in the launcher.

Launcher instrumentation was selected to provide information about the flowfield, especially the complex, viscous-inviscid interactions which resulted when the underexpanded rocket exhaust encountered the launcher wall. The locations of the 25 static-pressure gages are presented in Fig. 2. The position of the static-pressure gages, which were located in the vicinity of the change in cross section, are illustrated in the detailed sketches of the constrictions. Of the 4 static pressure gages located in the constriction itself, i.e., that portion of the launcher where the cross section was changing, only PS8 was operational for both geometries.

Flight Test Program

The run schedule for all 12 flights of the flight-test program is summarized in Table 1. For Flights 1 through 10, the constrictive change in cross section was accomplished by the modified rectangular step (Fig. 2a). For Flights 11 and 12, the change in cross section was accomplished by the 15° ramp (Fig. 2b). There were either no vent ports, two vent ports (which were located at $\bar{x}=82.99$ in.), or 4 vent ports (2 of

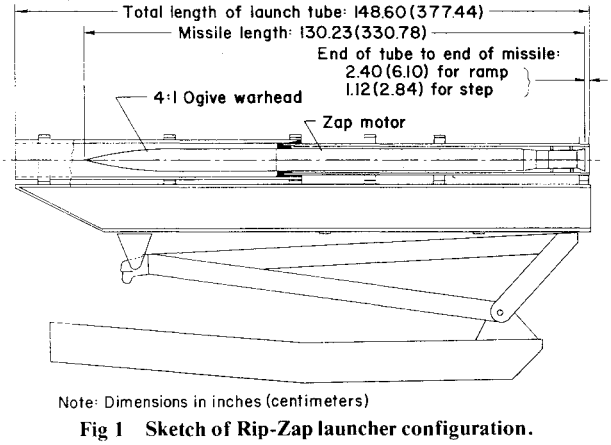

Fig 1 Sketch of Rip-Zap launcher configuration.

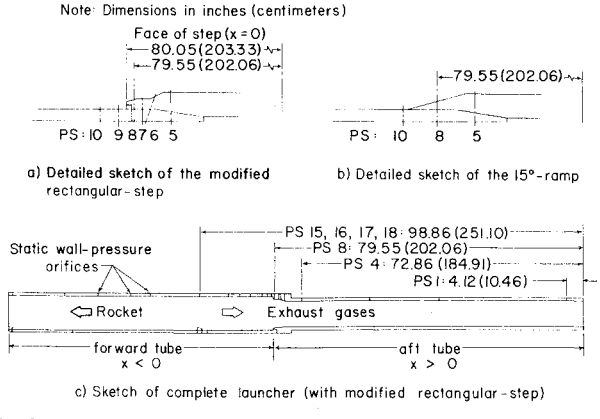

Fig. 2 Sketch of pressure instrumentation in the tube launcher used in the Rip-Zap program.

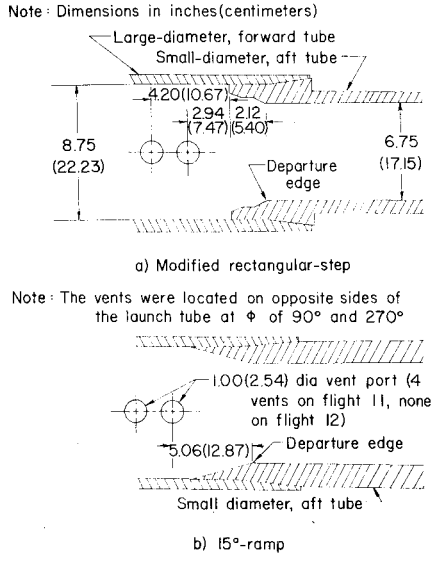

Fig. 3 Sketch of vent-port locations for the Rip-Zap launcher configuration.

which were located at $\bar{x}=82.99$ in. and two of which were located at $\bar{x}=84.25$ in.). The paired vent ports were diametrically opposed at ϕ of 90° and 270°. Sketches of the vent holes and their location are presented in Fig. 3. Referring to Table 1, there were: a) no vent ports for Flights 1, 2, and 12, b) 2 vent ports for Flights 3 through 8, and c) 4 vent ports for Flights 9, 10, and 11.

The pressure data from Flights 9 through 11, which utilized the instrumentation package described above, will be discussed here in detail. The data from Flights 1 through 8 (for which the launcher instrumentation was sparse) will be discussed only as necessary for correlations with the data from Flights 9 through 11. The pressure data for Flight 12 exhibited "anomlous" behavior during the time interval when the rocket exhausted into the large-diameter forward tube. Refer to Ref. 7 for a detailed discussion of the data from Flight 12 and additional data from other flights.

Discussion of Results

Rocket Position Histories

The location of the aft end of the rocket launcher for each of the 4 flights has been determined as a function of time using the output of the static wall-pressure gages. The experimentally determined nozzle-exit locations are presented in Fig. 4. The nozzle-exit position histories may be represented by one fairing for Flights 9 and 10 and another for Flights 11 and 12. The rocket arrived at a given position in the launcher approximately 4-6 msec earlier for Flights 9 and 10 than for Flights 11 and 12. The time differential existed even when the rocket was still in the small-diameter aft section of the launcher, i.e., before the rocket reached the cross-section change at an $\bar{x}_{ne}$ of approximately 80 in. (203 cm). Thus, the time differential is not attributed to the difference in the constrictive geometry of the launch tubes.

The position data were fit to a third-order polynomial and the coefficients determined for each flight. The curve fits (such as presented in Fig. 4 for Flights 9 and 11) were used to represent the nozzle-exit-position histories in the subsequent analysis. By using the nominal value of x_{ne}/r_{ne} as the independent variable rather than time, one can more readily see how geometric features of the launcher, such as the constriction, affect the pressures. Furthermore, the data for different flights can be compared, since time-dependent variation in configuration geometry, i.e., the location of the rocket with respect to the launcher, is "eliminated" (except for the differences between the actual and the curve-fit locations of the rocket for a given flight).

Typical Pressure Histories

The experimentally determined static wall pressures are presented in dimensionless form as the ratio p/p_{t1}, i.e., the static pressure divided by the stagnation pressure of the rocket chamber. The standard atmospheric pressure for the altitude of the White Sands Missile Range was used to convert the gage pressures to absolute values. The reservoir stagnation pressure was assumed to be 1400 psia (9.66×10^6 N/m^2). Dimensionless static pressure measurements are presented in Figs. 5-9 for selected gages (see Fig. 2). Data are presented for PS1, the first gage to be exposed to the rocket exhaust; for PS4, a gage near the internal end of the small-diameter aft tube; for PS8, the only gage in the constriction which was operational for both constrictive geometries, and for PS15

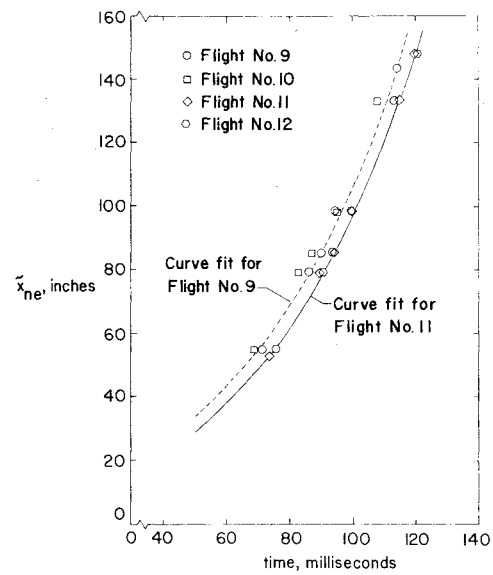

Fig. 4 Location of the aft end of the rocket as a function of time.

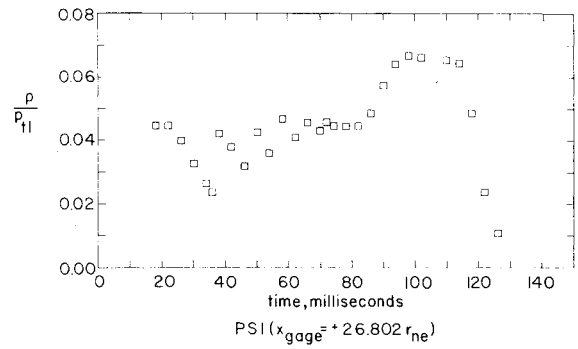

Fig. 5 Static pressure history for Flight 10.

Table 1 Summary of flight test program using constrictive stepped-tube launcher

Flight	Cross-section change	Instrumentation	Vent ports
1	Modified rectangular step	Limited static pressures	None
2	Modified rectangular step	Limited static pressures	None
3	Modified rectangular step	Limited static pressures	Two[b]
4	Modified rectangular step	Limited static pressures	Two[b]
5	Modified rectangular step	Limited static pressures	Two[b]
6	Modified rectangular step	Limited static pressures	Two[b]
7	Modified rectangular step	Limited static pressures	Two[b]
8	Modified rectangular step	Limited static pressures	Two[b]
9	Modified rectangular step	Launcher flow package[a]	Four[b]
10	Modified rectangular step	Launcher flow package[a]	Four[b]
11	15° ramp	Launcher flow package[a]	Four[b]
12	15° ramp	Launcher flow package[a]	None

[a] For the instrumentation and their locations, see Fig. 2.
[b] For the locations of the vent holes, see Fig. 3.

through PS18, gages located circumferentially at the same axial location in the large-diameter forward tube.

The static-wall-pressure measurements for PS1 are presented as a function of time for Flight 10 in Fig. 5 and as a function of the nondimensionalized nozzle-exit position, x_{ne}/r_{ne}, for Flights 9, 10, and 11 in Fig. 6. The character of the launcher flowfield which existed when the rocket exhausted into the small-diameter section, or aft tube, can be best seen in Fig. 5. The pressure recorded by PS1 periodically rose suddenly (due to a shock impinging on the wall),then decreased gradually. The period became shorter as the rocket accelerated away from the gage. Thus, these data are qualitiatively similar to the fully supersonic flows for statically fired rockets as reported by Batson[2] and for dynamically fired rockets as reported by Batson and Bertin.[3] The similarity between the pressure distribution for a statically fired rocket and that for a dynamically fired rocket results because the velocity of the exhaust gas is more than 20 times the velocity of the rocket as it leaves the launcher. Thus, the exhaust flow for the dynamic rocket launching is assumed to be quasi-steady.

As the exit plane of the rocket nozzle entered the large-diameter forward tube (at approximately 85 msec for Flight 10), the static pressure increased suddenly. Although the increase is evident in Fig. 5, the character of the pressure data is better illustrated by the parameters used in Fig. 6. The nozzle-exit position is a unique function of time, such that, as time increases (in Fig. 5), the nozzle-exit parameter x_{ne}/r_{ne}

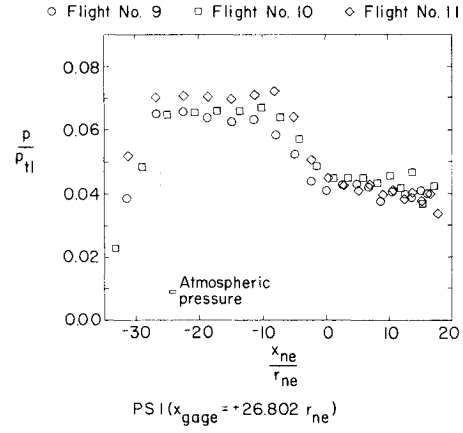

Fig. 6 Static pressure variation with nozzle exit position for an orifice in the small-diameter, aft tube far from the constriction.

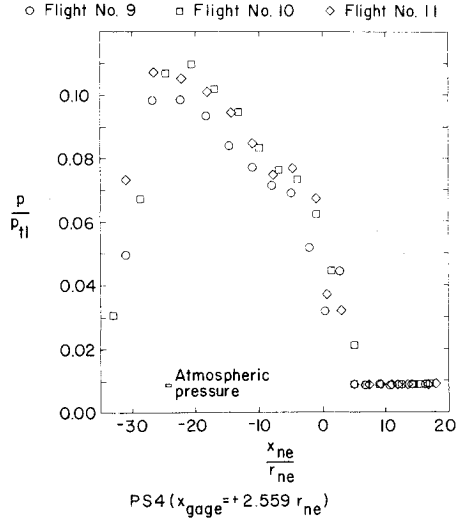

Fig. 7 Static pressure variation with nozzle exit position for an orifice in the small-diameter, aft tube near the constriction.

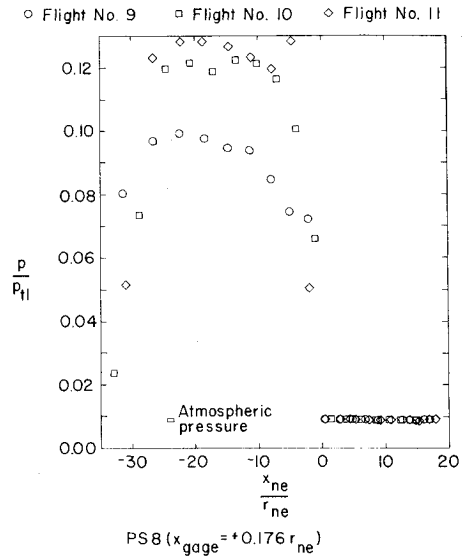

Fig. 8 Static pressure variation with nozzle exit position for an orifice located in the constriction.

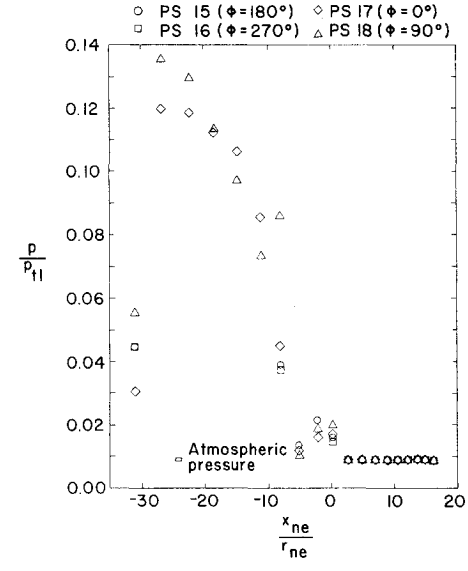

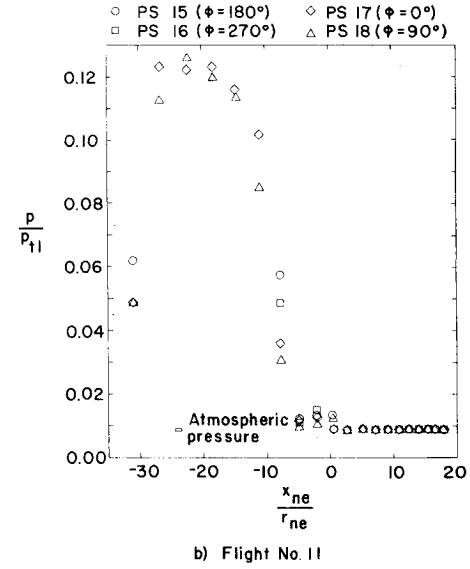

Fig. 9 A comparison of the static pressure histories for the 4 orifices located at $x_{gage} = -6.640\, r_{ne}$.

decreases from large positive values through zero and then to large negative values. Since the pressure parameter is the ratio of the experimentally determined static pressure to the assumed stagnation pressure, the flight-to-flight variations in the ratio p/p_{tl} may be due to differences between the actual stagnation pressure and the assumed value. When the rocket was 5 radii, or, more, into the large-diameter forward tube (i.e., $x_{ne} < -5.0\ r_{ne}$), the static pressure at PS1 (which was located far into the aft tube) was approximately constant. The magnitude of this constant pressure was the same whether the exhaust flow encountered the modified rectangular step (Flights 9 and 10) or the 15° ramp (Flight 11) before entering the aft tube. Thus, the variation in the geometry of the constriction did not significantly affect the downstream static pressure. Once the rocket had left the launcher, the static pressures recorded by PS1 decreased rapidly. The forward end of the launcher, for which $x_{ne} = -24.2\ r_{ne}$, is indicated by the atmospheric-pressure symbol.

The static wall-pressure measurements for PS4, which is in the aft tube near the constriction, are presented in Fig. 7 as a function of the dimensionless nozzle-exit location. The static pressure recorded by PS4 remained atmospheric until the rocket nozzle had passed the orifice. Based on the flowfield measurements from the cold-gas test program[5] when the static pressure in the annular region was significantly different from the atmospheric pressure, there was appreciable blowby flow. Thus, it is concluded that no significant blowby flow occurred as long as the rocket exhausted directly into the aft tube. Photographs of the launcher and the accelerating rocket support the conclusion that there was no blowby during this time period. When the rocket exhaust plane had passed the gage but still remained in the aft tube, the static pressure was approximately 0.04 p_{tl} (which is approximately the pressure recorded by PS1 while the rocket was in the aft tube). As the rocket passed the constriction (i.e., $x_{ne} \sim 0$) the pressure rose significantly, gradually reaching a constant value for Flights 9, 10, and 11. The constant value was not reached until the rocket exit plane was well into the forward tube. Because the pressures for Flights 10 and 11 were similar, it is believed that the geometric differences did not significantly affect the flow. Once the rocket exhaust plane cleared the launch tube, the pressure decreased rapidly.

The static-wall-pressure measurements for PS8, which is in the constriction, are presented in Fig. 8 as a function of the nozzle-exit location. As long as the rocket exhausted into the aft tube, the pressure remained constant, equal to the atmospheric value. The data for this gage are consistent with the previous observation that there was no significant blowby flow as long as the rocket exhausted directly into the aft tube. As the rocket exhaust impinged onto the constrictive surface of the launcher, the pressure in this region rose almost immediately. Despite the differences between the constrictive geometry for the two launchers, the pressure histories were essentially the same for Flights 10 and 11 (refer to Fig. 8). Thus, the differences in the geometry of the constriction did not have a significant effect on the static wall pressure. The differences in the pressure measurements for Flight 9 are attributed to experimental uncertainty.

When the rocket exhausted into the large-diameter forward tube, the pressure measurements in the vicinity of the constriction were more than 10 times the atmospheric pressure. Thus, there is a large pressure drop from the internal end of the forward tube (at the change in cross section) to the upstream end of the forward tube which exhausted to the atmosphere. As a result, there was a reverse, or blowby, flow in the annular region between the rocket and the wall of the forward tube. Photographs taken during Flights 9 through 11 verified the existence of a blowby flow. Using the photographs, the velocity of gas in the annular region was calculated to be approximately 500 fps.

The existence of a blowby flow was also evident in the static wall-pressure histories recorded by gages PS15, PS16, PS17, and PS18, all of which were located in the forward tube at $x_{gage} = -6.640\ r_{ne}$. Thus, with the exit plane of the nozzle near the constriction (i.e., $x_{ne} \approx 0$), these gages provide measurements of the static pressure in the annular region between the rocket and the tube wall. The pressure histories for these gages are presented in Fig. 9. The measurements for Flight 9 and for Flight 11 are presented to represent the flow in the launcher with the modified rectangular step and with the 15° ramp, respectively. For Flights 9 and 11 pressure measurements for gages PS15 and PS16 do not appear while the nozzle exit was in the region: $-10\ r_{ne} > x_{ne} > -25\ r_{ne}$. The gages for PS15 and PS16 saturated at approximately 100 psi and did not provide meaningful data while the rocket was in this region.

As the exit plane of the rocket nozzle passed the constriction and entered the forward tube ($0\ r_{ne} > x_{ne} > -2.5\ r_{ne}$), the pressure recorded by these gages rose, indicating the occurence of significant blowby flow. The pressure increase

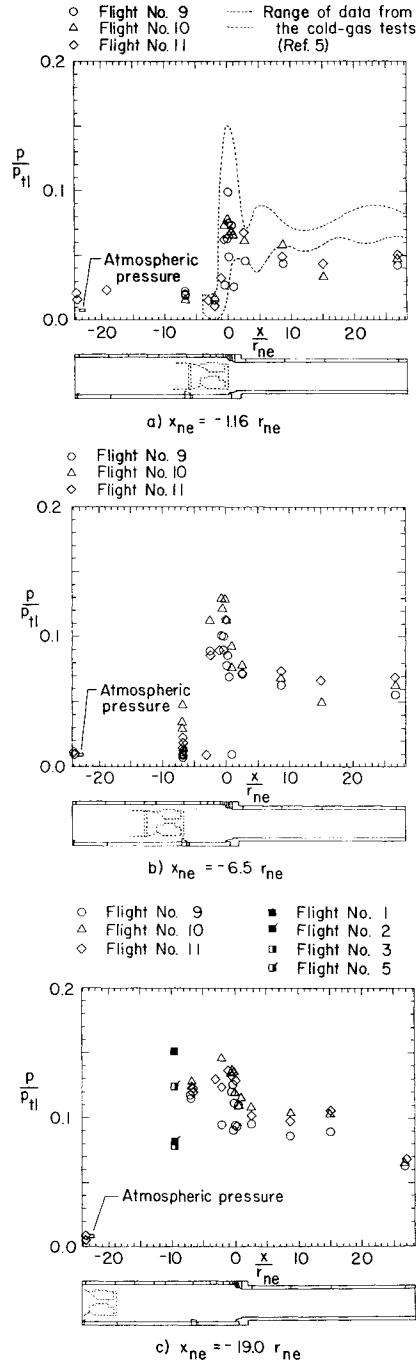

Fig. 10 Static wall-pressure distributions along the tube launcher.

was greater for the launcher with the modified rectangular step, i.e., Flights 9 and 10. When the exit plane of the cold-gas nozzle was within 2.5 r_{ne} of the step, the blowby flow from the cold-gas tests[5] was greater for a rectangular-step configuration than for a 15° ramp. Thus, the Rip-Zag launch data presented in Fig. 9 are consistent with the results for the cold-gas flows. As the rocket moved further from the step ($-2.5\ r_{ne} > x_{ne} > -6.0\ r_{ne}$), the pressure recorded by these four gages decreased. Based on the previous discussion, the observed pressure decrease indicated that the blowby flow rate decreased. Thus, as the rocket nozzle was moving away from the step, but had not yet reached the gage, the magnitude of the reverse flow increased and then diminished. The varying strength of the blowby flow with the rocket nozzle in this region might be described as a "puff." For the cold-gas tests, the maximum blowby flow rate for the rectangular step occurred when $x_{ne} = -0.75\ r_{ne}$. The blowby flow rate decreased as the nozzle moved farther from the step. For the 15° ramp configuration, the blowby flow rate for the cold-gas tests had not begun to decrease with distance, but data were available only for $0 > r_{ne} \leq -2.55\ r_{ne}$.

When the rocket passed the plane of these gages such that the exhaust flow impinged directly on them, the pressure rose dramatically. The pressure downstream of the impingement shock was approximately 0.12 p_{tl}, which was approximately 13 atm. Recall that, when the rocket exhausted into the small-diameter aft tube, the pressure downstream of the impingement shock was approximately 0.04 p_{tl}. Numerical solutions of the underexpanded exhaust (from a stationary rocket) impinging on the tube wall show that the pressure downstream of an oblique impingement shock would be less for the larger-diameter tube. The static wall pressure immediately downstream of the impingement shock wave was calculated to be 0.0529 p_{tl} for the forward tube ($r_t = 1.54\ r_{ne}$) and 0.0667 p_{tl} for the aft tube ($r_t = 1.19\ r_{ne}$). The numerical calculations assume that the rocket exhaust expands from the theoretical value of the exit-plane pressure to the base pressure, which is atmospheric for these flows. Thus, in the theoretical solution the flow which impinges on the wall is turned approximately 30-35° by a weak, oblique shock wave. The fact that the experimentally recorded pressures were so much greater when the rocket exhausted into the larger-diameter forward tube suggests that the flow contained a strong, normal shock wave and was, therefore, not fully supersonic. This conclusion is supported by the cold-gas data of Ref. 6.

Static-Wall-Pressure Distributions

Pressure data such as those presented in Figs. 6-9 were used to construct the static-wall-pressure distributions for several nozzle-exit locations. As noted previously, the static wall pressures were essentially the same for both constrictive geometries (Fig. 2). Therefore, the distributions for the three flights are presented in Fig. 10. Included for comparison are pressure measurements from the first Rip-Zap flight-test program[4] and from the cold-nitrogen test program.[5] Also presented in each figure is a sketch of the launcher (with the modified rectangular step), the instrumentation locations, and the aft end of the rocket.

Consider the pressure distributions obtained with the exit plane of the rocket nozzle in the forward tube but relatively near the constriction, e.g., $x_{ne} = -1.16\ r_{ne}$ in Fig. 10a. The pressure distribution is that which was obtained during the time that the flowfield in the launcher changed from the fully supersonic flow generated when the rocket exhausted into the aft tube to the primarily subsonic flow generated when the rocket had moved well upstream of the constriction. The data from the dynamic rocket launchings were in reasonable agreement with the data from the cold-gas tests in which the nozzle was stationary.[5] As noted previously, the exhaust flow for the rocket launching is assumed to be quasi-steady. Downstream of the nozzle, the pressure increased rapidly as the exhaust impinged on the wall,and reached a maximum at the constriction. The static pressure measurements from the orifices located in the aft tube were lower than the values at the constriction. The streamwise variations of the static pressure in the small-diameter aft tube are attributed to the reflection of oblique shock waves (which implies that the flow remained fully supersonic). However, these data by themselves would not be conclusive as to whether the flow in the aft tube was subsonic or supersonic. To support the conclusion that flow in the aft tube remained supersonic for $x_{ne} = -1.16\ r_{ne}$, compare the data of Fig. 10a with that of Fig. 10c. The pressures measured in the aft tube with $x_{ne} = -1.16\ r_{ne}$ were low compared to the values obtained when the nozzle was farther from the constriction ($x_{ne} = -19.0\ r_{ne}$) where the flow in the aft tube was clearly subsonic.

The static pressures in the annular region were significantly above the atmospheric level. As previously discussed, the static wall pressures from the annular region indicate considerable blowby flow. The existence of significant blowby flow is consistent with the cold-gas data.

Consider next the static-wall-pressure distributions with the exit plane of the rocket nozzle well into the forward tube, $x_{ne} = -19.0\ r_{ne}$ in Fig. 10c. The distributions for Flights 9, 10, and 11 are essentially the same. Downstream of the nozzle exit-plane, the pressures rose sharply due to the impingement shock wave, remained essentially constant in the forward tube from the shock wave to the constrictive change in cross section, decreased at the constriction, and remained essentially constant along the length of the small-diameter aft tube. The magnitude of the pressure increase at impingement indicates that the shock wave was relatively strong. Furthermore, the pressure decrease at the constriction indicates that the flow accelerated. Recall that, when the area decreases, subsonic flow accelerates while supersonic flow decelerates. The results of the cold-gas test program at the University of Texas at Austin[6] indicate that the generation of the normal shock wave resulted because the flow choked at the constriction.

Also included in Fig. 10c are the relevant pressure data from the earlier Rip-Zap flight-test program.[4] For Flights 1 and 2, there were no vent ports; for Flights 3 and 5, there were two vent ports; and for Flights 9, 10, and 11, there were four vent ports. It was difficult to determine accurately the pressure at a particular time using the data as presented in Ref. 4, since the pressure was graphed to an extremely small scale, e.g., 300 psi/in. Within the uncertainty, the pressure measurements were essentially equal for Flights 1, 2, 3, and 5, and were equal to the measured values from Flights 9, 10, and 11. Thus, the static wall pressures in the launch tube were not significantly affected by the presence (or absence) of vent ports. This is also the conclusion based on cold-gas test data obtained at the University of Texas at Austin.[6] It should be noted, however, that the presence of vent ports near the constriction reduced the blowby mass-flow rate. Because the pressure in the large-diameter forward tube was much greater than the atmospheric value, the flow through the vent ports was choked. Therefore, the mass-flow rate of the vented gas increases in direct proportion to the area of the vent ports and produces a corresponding decrease in the blowby flow rate.

It is not possible to describe the flow in the launcher when $x_{ne} = -6.5\ r_{ne}$ using only the data presented in Fig. 10b. However, if one includes the data for other nozzle positions, one concludes that the flowfield in the launcher was similar to that described for Fig. 10c. The constrictive geometry caused the flow to choke, so that a normal shock wave was generated just downstream of the rocket exit. For the orifices located circumferentially near the exit plane (i.e., $x_{gage} = -6.640\ r_{ne}$), the pressures for Flight 10 appear to be relatively high. The nozzle exit plane for Flight 10 may actually have been slightly farther into the forward tube than given by the curve-fit location, so that the static pressure at $-6.640\ r_{ne}$ was respond-

ing to the exhaust impingement. Thus, the relatively large data scatter for this orifice is attributed to the use of a curve fit of the measurements to define the nozzle exit-plane location (Fig. 4).

Conclusions

Launcher flowfield data from the rocket launchings conducted at the White Sands Missile Range have been discussed. A quantitative understanding of the launcher flowfield which results when a rocket exhausts into a constrictive-step-tube launcher has been constructed using static-wall-pressure distributions, pitot-pressure measurements, and flowfield photographs. Based on these data, the following comments are made regarding the flowfield as a function of the nozzle-exit location:

1) When the exit plane of the rocket nozzle was in the small-diameter aft tube the flow was fully supersonic. There was not significant reverse (or blowby) flow.

2) When the exit plane of the rocket nozzle passed the constriction, the pressures measured at the orifices downstream of the nozzle increased significantly. The pressures measured at the orifices upstream of the nozzle increased, then decreased, indicating the occurrence of a blowby flow of varying strength. The differences between the two constrictive geometries did not significantly affect the pressure measurements.

3) When the exit plane of the rocket nozzle moved away from the constriction, the pressure for a particular orifice downstream of the nozzle rose, reaching a relatively high, "constant" value. With the rocket in the large-diameter forward tube, the static wall pressure downstream of the impingement shock was much higher than when the rocket was in the small-diameter aft tube. Thus, the flow downstream of the impingement shock was apparently subsonic. The upstream static-pressure data (from orifices located in the annular region) indicated the occurrence of the reverse flow.

For the geometries tested, the variations in the number of vent ports or in the geometry of the constriction had no significant effect on the static-wall-pressure distributions. However, the blowby mass-flow rates would be affected by variations in the number of vent ports. Changes in the vent-port geometry greater than those of the present tests could produce corresponding changes in the flowfield in the launcher. Furthermore, if parameters such as the ratio of aft-tube radius: forward-tube radius: nozzle-exit radius were changed significantly, the conclusions could be radically changed.

References

[1] Fabri, J. and Siestrunk, R., "Supersonic Air Ejectors," *Advances in Applied Mechanics*, Vol. V. Academic Press, New York, 1958, pp. 1-34.

[2] Batson, J. L., "Study of the Flowfield Produced by an Axisymmetric Underexpanded Jet Exhausting into a Cylindrical Tube," Ph. D. thesis, Department of Aerospace Engineering and Engineering Mechanics, Dec. 1972, University of Texas at Austin, Austin, Texas.

[3] Batson, J. L. and Bertin, J. J., "Experimental Study of Flowfield Produced When an Underexpanded Rocket Exhausts into Cylinder Tube," AIAA Paper 73-1227, Las Vegas, Nev., 1973.

[4] "Feasibility Flight Testing of Rocket Impelled Projectile (RIP)," Report 7-52100/3R-5, 1973, LTV Aerospace Corp., Michigan Division.

[5] Bertin, J. J., Horn, M. K., and Webber, T. L., "Experimental Study of Flow Field Produced When an Underexpanded Jet Exhausts into a Constrictive Stepped Launch Tube," Aerospace Engineering Rep. 74002, Jan. 1974, University of Texas at Austin, Austin, Texas.

[6] Morris, R. R., Garms, E. M., Faria, H. T., and Motal, M. R., "Experimental Study of an Underexpanded, Supersonic Nozzle Exhausting in a Constrictive Launch Tube," Aerospace Engineering Rep. 75001, April 1975, University of Texas at Austin, Austin, Texas.

[7] Bertin, J. J. and Reiman, R. A., "Analysis of the Launch-Tube Flowfield for Rip-Zap Firings," Aerospace Engineering Rep. 74005, Oct. 1974, University of Texas at Austin, Austin, Texas.